Anal. Chem. **2008,** *80,* 2524−2530

Charge Monitoring Cell Mass Spectrometry

Wen-Ping Peng,[†,#] Huan-Chang Lin,[†] Ming-Lee Chu,[‡] Huan-Cheng Chang,[§] Hsin-Hung Lin,[†] Alice L. Yu,[†] and Chung-Hsuan Chen*[,†]

Genomics Research Center, Institute of Physics, and Institute of Atomic and Molecular Sciences, Academia Sinica, Taipei, Taiwan, Republic of China

An instrument to directly measure the charge carried by a cell or a microparticle as well as mass-to-charge ratio of the cell/microparticle was developed for rapid mass distribution measurement. A successful mass spectrum with a record high mass has been demonstrated. In this article, the details of the construction and operation of the charge monitoring cell mass spectrometer are reported. Examples are also given for demonstration and discussion.

Recently, detection of very large bioparticles such as viruses and cells has aroused great interest.[1] Up to now, only a few methods have been reported for cell measurement. For example, antibody-conjugated nanoparticles were used to identify bacteria[2] and micromechanical oscillators were used for single-cell detection.[3] Novel mass spectrometry offers new approaches to take the challenge with technology development in ion mobility mass spectrometry,[4,5] time-of-flight mass spectrometry,[6,7] and ion trap time-of-flight mass spectrometry.[8,9]

Up to now, nearly all mass spectrometers can only measure mass-to-charge ratios (m/z). For small molecules, charge (z) is usually equal to one. Therefore, mass (m) can be determined. For electrospray mass spectrometry, the number of the charge is usually higher than one, and large biomolecular ions usually have a distribution of the number of charges. Mass determination is often determined by the series of peaks representing different numbers of charges from the same type of molecule. Nevertheless, electrospray is not suitable to analyze samples with a mixture of a large number of biomolecules without preseparation due to the complexity of spectra. When a particle does have a very high mass, more than hundreds of electrons can be present on one particle of interest. Determination of the number of charges becomes very difficult and impractical. In addition to the problem of charge determination, the method to detect the particle with a very high m/z is also limited. For example, a charge amplification device such as a microchannel plate (MCP) becomes very inefficient when particle m/z reaches 1 000 000 and kinetic energy is less than 30 000 eV.[10]

Time-of-flight mass spectrometry with direct charge measurement to measure particles with the mass range of mega-Daltons has been reported.[11] It is convenient to use handy electronics to measure the number of charges and to detect the arrival time of a charged particle simultaneously. Nevertheless, the reported mass resolution is low[11] even when ultralow noise electronics are used. A few hundred charges carried by a single particle with the electronics noise of ∼50 electrons have been reported.[6] The signal-to-noise ratio does become the limiting factor in the determination of a particle mass. Recently, we increased the mass range for the ion trap with lower rf frequency. At the same time, a condition to enhance the charge number on the particles in interest was developed. In combination of all these, a mass spectrometer using simple homemade electronics can be operated with a good efficiency to achieve a record high-mass measurement. In this article, the details of this charge monitoring mass spectrometer with ion trap and charge enhancement are reported. Sample measurements to cross-examine the performance of the mass spectrometer are presented and analyzed. More detailed benefits and other possible applications are also discussed.

Instrumentation. The schematic of the charge monitoring cell mass spectrometer (CMCMS) is shown in Figure 1. The purpose of building the CMCMS is to be able to measure the masses of cells/microparticles with high speed. For this device, cell or microparticle samples are deposited onto a Si wafer. Laser-induced acoustic desorption (LIAD) is used to desorb cells/microparticles into the ion trap. The m/z ratios of the cells are determined by scanning the trapping frequency to eject charged cells. A Faraday disc is used to measure the number of charges (z) on the particle so that the mass of the charged particle can be

* To whom correspondence should be addressed. E-mail: winschen@gate.sinica.edu.tw.

[†] Genomics Research Center.

[‡] Institute of Physics.

[§] Institute of Atomic and Molecular Sciences.

[#] Present address: Department of Physics, National Dong Hwa University, Hua-Lien, Taiwan, Republic of China.

(1) Siuzdak, G.; Bothner, B.; Yeager, M.; Brugidou, C.; Fauquet, C. M.; Hoey, K.; Change, C.-M. *Chem. Biol.* **1996**, *3*, 45−48.

(2) Zhao, X.; Hilliard, L. R.; Mechery, S. J.; Wang, Y.; Bagwe, R. P.; Jin, S.; Tan, W. *Proc. Natl. Acad. Sci. U.S.A.* **2004**, *101*, 15027−15032.

(3) Llic, B.; Czaplewski, D.; Zalalutdinov, M.; Craighead, H. G.; Neuzil, P.; Campagnolo, C.; Batt, C. J. *Vac. Sci. Technol., B* **2001**, *19*, 2825−2828.

(4) Thomas, J. J.; Bothner, B.; Traina, J.; Benner, W. H.; Siuzdak, G. *Spectroscopy* **2004**, *18*, 31−36.

(5) Hogan, C. J., Jr.; Kettleson, E. M.; Ramaswami, B.; Chen, D.-R.; Biswas, P. *Anal. Chem.* **2006**, *78*, 844−852.

(6) Fuerstenau, S. D.; Benner, W. H.; Thomas, J. J.; Brugidou, C.; Bothner, B.; Siuzdak, G. *Angew. Chem., Int. Ed.* **2001**, *40*, 542−544.

(7) Tito, M. A.; Tars, K.; Valegard, K.; Hajdu, J.; Robinson, C. V. *J. Am. Chem. Soc.* **2000**, *122*, 3550−3551.

(8) Peng, W.-P.; Yang, Y.-C.; Kang, M.-W.; Tzeng, Y.-K.; Nie, Z.; Chang, H.-C.; Chang, W.; Chen, C.-H. *Angew. Chem., Int. Ed.* **2006**, *118*, 1423−1426.

(9) Nie, Z.; Tzeng, Y.-K.; Chang, H.-C.; Chiu, C.-C.; Chang, C.-Y.; Chang, C.-M.; Tao, M.-H. *Angew. Chem., Int. Ed.* **2006**, *45*, 8131−8134.

(10) Geno, P. W.; MacFarlane, R. D. *Int. J. Mass Spectrom. Ion Processes* **1989**, *92*, 195−210.

(11) Karas, M.; Ingendoh, A.; Bahr, U.; Hillenkamp, F. *Environ. Mass Spectrom.* **1989**, *18*, 841−843.

10.1021/ac7024392 CCC: $40.75
Published on Web 03/06/2008

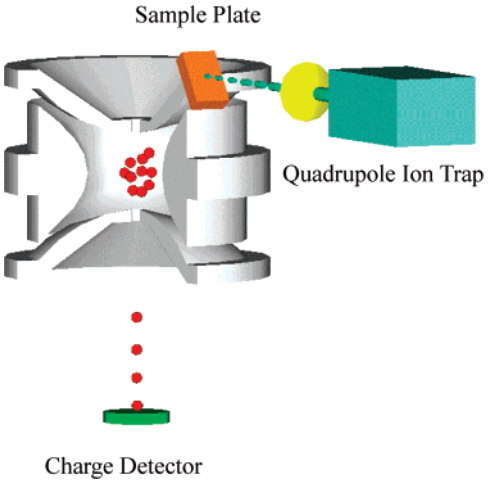

Figure 1. Schematic of the experimental setup of the charge monitoring cell mass spectrometer (CMCMS), which includes a quadrupole ion trap (QIT), a pulsed YAG laser, and a charge detector.

determined. There are a few specific features for CMCMS compared to most conventional commercial mass spectrometers. They include (1) LIAD to desorb charged particles into the quadrupole ion trap (QIT), (2) a very high m/z ratio can be obtained using a frequency scan which operates in mass-selective instability mode, (3) direct measurement of the number of charges (z) on a particle without secondary electron amplification, and (4) a corona discharge to enhance the number of charges onto a microparticle. These specific features will be reported in the following.

Laser-Induced Acoustic Desorption. Laser-induced acoustic desorption was originally developed for biomolecule detection without the need of matrix.[12−14] Recently, we applied LIAD to successfully desorb cells, viruses, and microparticles with good efficiencies.[8,9,15,16] To prepare the sample for LIAD, an aliquot (5 μL) of the purified particle suspension (containing $\sim 1 \times 10^7$ particles/mL) was deposited onto an $\sim$400 μm thick Si wafer and dried under a desiccated box. The air-dried Si wafer was then positioned in the gap between the ring and endcap electrodes ($2r_0 = 19.97 \pm 0.02$ mm) of the QIT. A frequency-doubled pulsed Nd:YAG laser (Laser Technique, Berlin, Germany) at 532 nm with the laser energy at 30 mJ/pulse was used to irradiate the sample from the back side of the wafer. The laser duration was $\sim$6 ns, and the power density on the Si wafer ranged from 1 to $\sim 5 \times 10^8$ W/cm^2. The strong absorption of laser photons induced an acoustic wave to cause particle desorption from the opposite side.[13] Desorbed charged particles were captured by the ion trap driven by a home-built audio frequency power amplifier applied to the ring electrode (two endcaps were grounded to ensure good shielding of charge detector electronics) and damped to the trap center by helium buffer gas at $\sim$70 mTorr.

(12) Golovlev, V. V.; Allman, A. L.; Garrett, W. R.; Taranenko, N. I.; Chen, C. H. *Int. J. Mass Spectrom. Ion Processes* **1997**, *169/170*, 69−78.
(13) Golovlev, V. V.; Allman, S. L.; Garrett, W. R.; Chen, C. H. *Appl. Phys. Lett.* **1997**, *71*, 852−854.
(14) Campbell, J. L.; Fiddler, M. N.; Crawford, K. E.; Gqamana, P. P.; Kenttamaa, H. I. *Anal. Chem.* **2005**, *77*, 4020−4026.
(15) Peng, W. P.; Lin, H. C.; Lin, H. H.; Chu, M. L.; Yu, A. L.; Chang, H. C.; Chen, C. H. *Angew. Chem., Int. Ed.* **2007**, *46*, 3865−3869.
(16) Peng, W.-P.; Lee, Y. T.; Ting, J. W.; Chang, H. C. *Rev. Sci. Instrum.* **2005**, *76*, 023108(1−4).

Corona Discharge and Trapping. A pressure-controlled corona discharge was important in this study since it enhanced the number of charges on a cell/microparticle. Without the corona discharge, only tens to hundreds of charges can be obtained during LIAD for a single particle measurement of red blood cells.[8] In this work, the He pressure was controlled to lead to high-voltage discharge during the laser desorption process. Clear blue and white discharge plasma was observed between the ion trap and desorption plate during the time the laser beam shined on the back side of the Si wafer. The discharge typically lasted for $\sim$1 s, and the rf voltage was set at $\sim$3000 V_{p-p}. During discharge, the charge detector (see later section) could pick up some ions produced. A typical waveform taken with the charge detector is shown in Figure 2. The limiting condition to the discharge is the high-voltage breakdown between ion trap electrodes. Usually breakdown started as the pickup of the charge detector reached about 1 V signal. Typical base pressure used in this experiment was about 50−150 mTorr to allow the mild discharge without breakdown. The measured charge number on 15 um particles under various pressures is shown in Figure 3. While the pickup signal of the ac field was quite large on the charge detector when the pressure was high during laser desorption, the pickup signal was absent when the pressure was pumped low after the particle trapping operation was finished.

Trapping of particles was accomplished by properly adjusting the LIAD laser energy ($\sim$20 mJ/pulse), trap-driving frequency (Ω), as well as voltage amplitude (V_{ac}). The ion trap was operated under an axial mass-selective instability mode by scanning trap-driving frequency with the sweeping range from 350 to 20 Hz. A voltage of 1520 V was initially applied with a high-voltage transformer driven by an audio frequency power amplifier and a functional generator. By simply scanning the audio frequency from a functional generator, particles were ejected along the axial direction, and the number of charges on each particle was subsequently detected by a Faraday disc charge collector. The mass of each particle was determined according to the measurements of m/z and z for the particle. The frequency scan mode was adopted in this experiment; it is necessary to have an accurate measurement of rf frequency so that the m/z can be calculated. Thus, a high-precision averaging peak-to-peak voltage detector built in-house was used to constantly measure V_{ac} throughout the entire experiment.[16]

Charge Detector. We have estimated the particle speed using sinusoidal particle motion. Particles with angular frequency ω and amplitude z_0 have a maximum speed of ωz_0 (when the particle is at the $z = 0$). $z_0 = 1$ cm of the QIT size is used. The operation frequency of the QIT was between 300 and 50 Hz for the large particles. From these numbers, the estimated particle speed should be below 20 m/s when the particle exits from the QIT. The image charge collection time of a large particle is estimated to be in the scale of milliseconds assuming the Faraday disc starts to "see" the charge when the particle is about 1 cm away from it. The long charge collection time limited our choice with commercial charge amplifiers. A homemade charge detector circuit with long discharge time constant was designed to allow the proper integration of the image charge of the particle. The details of the charge detector and one sample of the waveform scanned are shown in Figure 4. The detector board was designed to be

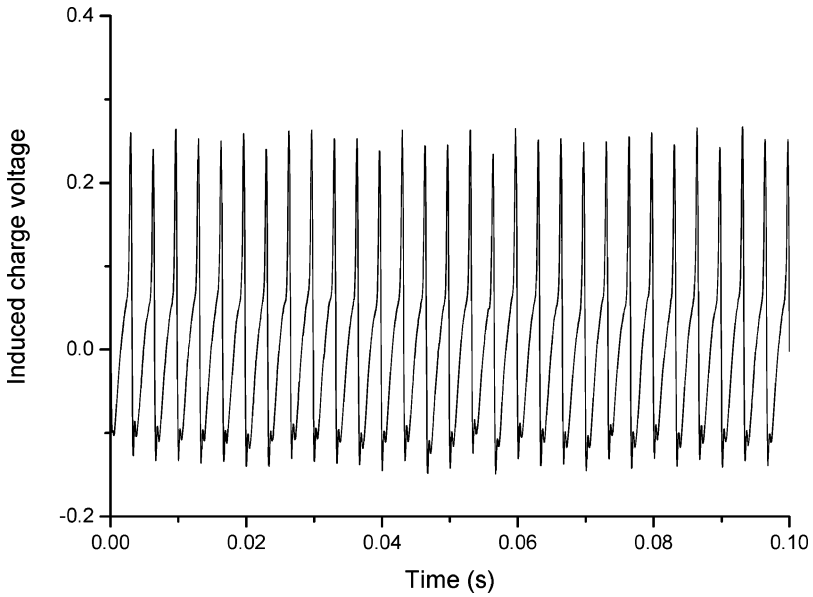

Figure 2. Corona discharge is induced by leaking the He buffer gas into the ion trap chamber; the corona discharge signal can be detected by the charge detector above 50 mTorr.

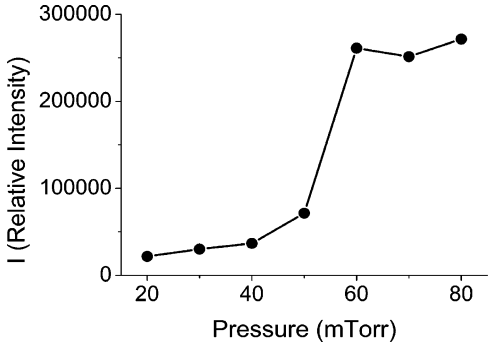

Figure 3. Enhancement of charge attached to a 15 μm microparticle. Significant enhancement can be clearly seen starting at 50 mTorr.

mechanically compatible to the ion trap. A circular metal disc in the center of the detector board acted as a Faraday disc to collect the image charge induced by particles. The Faraday disc is less than 1 cm away from the exit hole of the ion trap when the detector is mounted under the ion trap. A stainless mesh with >90% transmission was placed between the Faraday disc and the exit hole of the ion trap to shield the ac field of the ion trap voltage. The diameter of the Faraday disc was 1 cm which should be sufficient to cover all the particles that came out of the ion trap. The first stage of the charge detector circuit was a charge integrator which included a low-noise JFET and a low-noise operational amplifier. The 1 pF C1 capacitor determined the charge to voltage conversion ratio. R7 and R8 provided a voltage gain of 4. The value R6 $\times$ C2 determined the discharge time constant as 10 ms. The second stage voltage amplifier provided a gain of 40 and with a simple band-pass filter for the filtering of both high-frequency and low-frequency noise. In general, the output of the second stage amplifier provided a sufficient pulse amplitude to the ADC (analog to digital converter) at the outside of the vacuum chamber. A typical mass spectrum from the CMCMS is shown in Figure 5 when the charge detector was used to work with the QIT.

The gain calibration of the charge detector was performed in two different levels. They include (1) the relative gain calibrated with an electronic pulse and (2) the absolute gain with particles of a known mass. Electrical calibration was carried out by applying an electrical pulse of known amplitude and shape to the "test pulse input" connector as indicated in Figure 4. The test pulse voltage was attenuated by R4 and R5 to 1/100, then fed to C2 (1 pF). The other terminal of C2 was virtually grounded to the amplifier input. The charge injection ratio was 10 fC (about 63 000 e)/V from the test input. The test pulse calibration gave the charge conversion gain of about 1 mV/50 e. The measured noise of the charge amplifier, 10 mV (rms), then corresponded to about 500 e rms noise. The timing factor needed to be considered since the discharge time constant of 10 ms was not much longer than the charge collection time of real particles (ranging from 1 to 8 ms). Figure 4c shows the timing factor calibration taken with the test pulse with different leading edges. The electrical calibration was quite handy, however, not very precise, mainly because that the uncertainty of the two small 1 pF capacitors C1 and C2. Capacitors with this small value were hard to produce precisely. In addition, other circuit elements could easily add up considerable amount of parasitic to the actual capacitor value. This uncertainty caused by an electrical component was estimated to cause probably 20% gain error. This error is a fix factor to the calibrated value, fixed but hard to determine. The key parameters determined by electrical calibration are listed in Table 1.

It is essential to have particles of known mass to perform absolute calibration to the charge detector. We have used particles with narrow size distribution obtained from NIST as our standard mass. The largest particles with a certificate from NIST are polystyrene particles with nominal 3 μm diameter. The standard mass m could be estimated with the density and diameter of the particle. These standard particles were scanned using QIT. The ejection frequency gives the m/z of each particle. The charge number on each particle was obtained with m/z and standard mass value m.

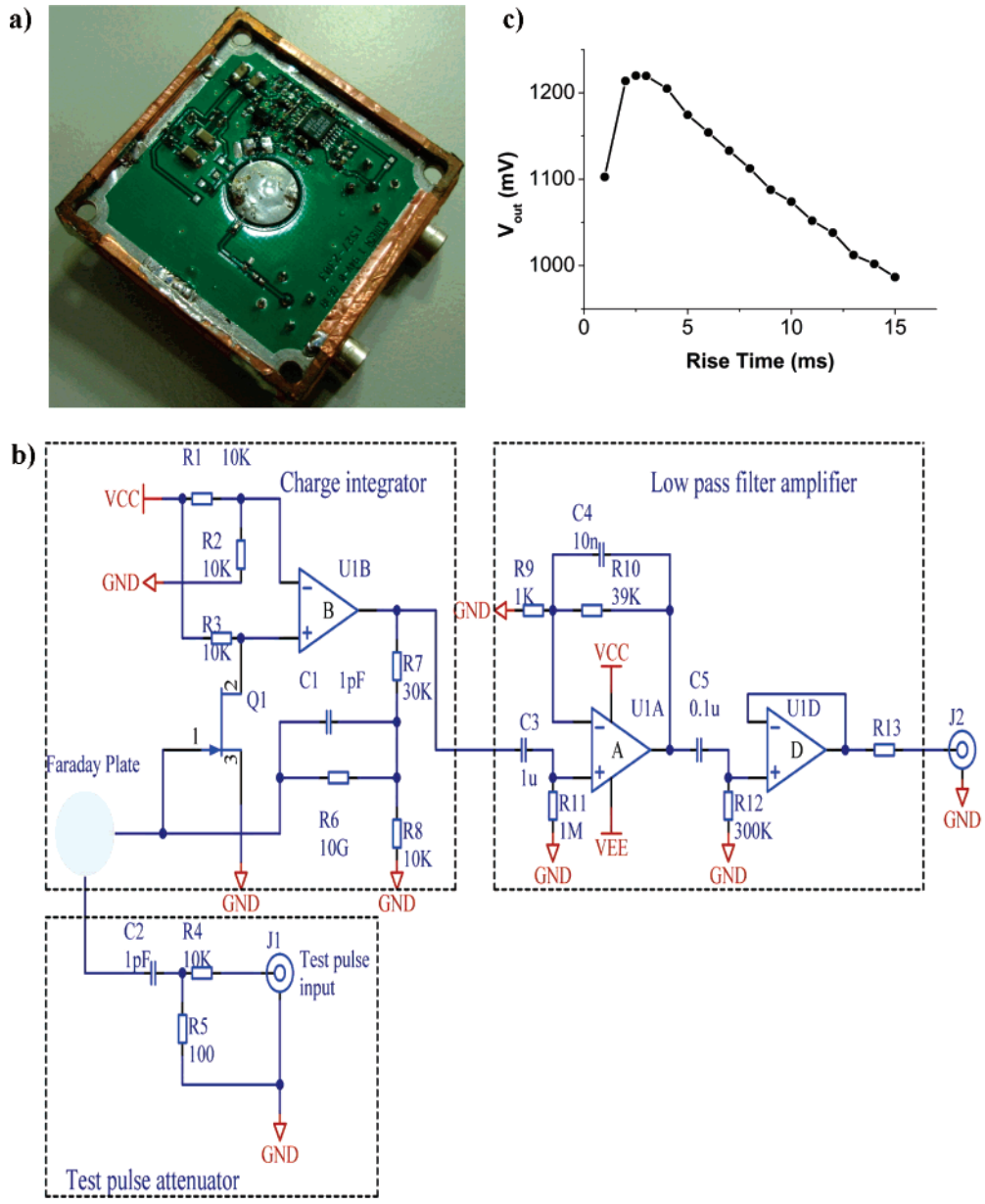

Figure 4. Circuit design of the charge detector: (a) components are arranged in a 44 mm by 44 mm PCB board; (b) electronic schematic; (c) pulse height correction factor vs pulse leading edge time.

Visible Monitoring of Trapped Cells/Microparticles. Visible monitoring is not necessary but just for convenience to ensure cells/microparticles are getting trapped. A He−Ne laser (632 nm and 15 mW) was occasionally shined through the gap between the ion trap electrodes to illuminate the trapped cells/microparticles. The resulting scattered laser light was collected at a 55° forward angle and guided to a digital electron multiplier charge-coupled device (DEMCCD) camera connected to the computer. Once the trapping process can be assured, both the He−Ne laser and CCD camera are no longer essential.

EXPERIMENTAL SECTION

Material Preparation. Polystyrene microparticles with the size of 15 and 3 μm were obtained from Sigma-Aldrich and NIST, respectively. Polystyrene spheres were thoroughly washed with deionized water, recovered by centrifugation, and resuspended in filtered (0.2 μm pore size filter) distilled water. This purification step is important because the presence of sodium azide or any residual salt components could inadvertently produce background particles during laser desorption so that analysis becomes difficult.

The Jurkat human T-lymphocytic leukemia cells were obtained from ATCC (Rockville, MD) and maintained in RPMI 1640 medium (Gibco Life Technologies, New York, NY) containing 1% standard penicillin/streptomycin (10.000 IU/mL), 2 mM L-glutamine, and 10% fetal bovine serum. All cells were grown in a humidified incubator at 37 °C and 5% CO_2. The cell line Jurkat was washed with Dulbecco's phosphate-buffered saline (PBS, Gibco BRL) and fixed with 4% formaldehyde in PBS for 15 min at room temperature. Thereafter, the cells were washed three times in distilled deionized water, then counted and resuspended in distilled deionized water.

Precaution on Data Taking. In order to ensure the measurements of cells/microparticles in the samples not particles desorbed

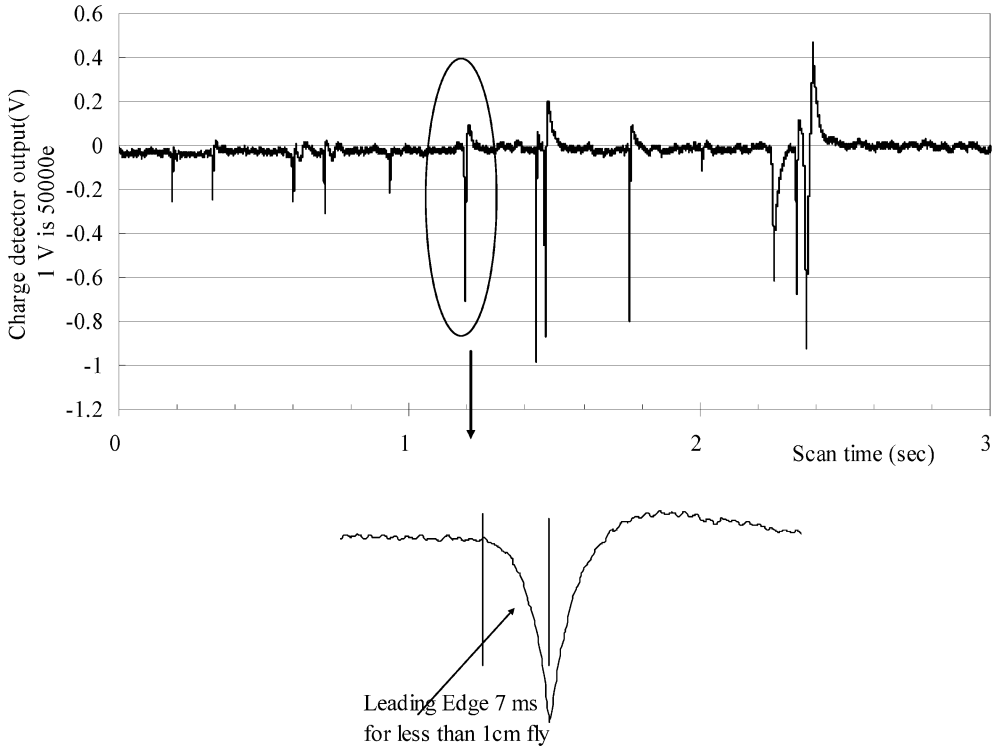

Figure 5. Mass spectrum of Jurkat cancer cell. Each peak indicates a cell particle, and the peak height is the number of charges on the particle. The mass of each cell was calculated from simultaneous measurement of mass-to-charge ratio (m/z) and the number of charges (z). The expanded single-particle pulse shows the leading edge of the pulse. This leading edge corresponds to a fly speed of about 1 m/s.

Table 1. Key Parameters of the Charge Detector

charge conversion ratio	~50 electrons/mV
noise voltage	~10 mV rms
equivalent noise electron	~500 e rms
integrator discharge time constant	~10 ms

from the Si surface due to the acoustic desorption, a blank reference was tested. No scattered laser light to indicate the existence of particles was detected in the control experiments using pure water dropped onto the Si wafer. Therefore, it confirms that the observed signals were indeed derived from desorbed polystyrene spheres or cells by acoustic desorption rather than from dust particles in water and/or on the surface. In general, there were about 10^6 to ~10^7 microparticles/cm^2 placed on the Si wafer substrate. The sample lasted for 30 laser pulses for desorption, and more than 10 particles were trapped for each laser pulse. With the laser beam focused to ~1 mm, the trapping efficiency was estimated as a few percent.

RESULTS AND DISCUSSION

A typical mass spectrum of Jurkat cell by CLIAD-MS is shown in Figure 5. Each peak indicates a specific m/z determined by the ejection frequency and voltage. The number of charges on each cell was derived by the amplitude obtained from the Faraday disc. Mass and charge distributions for polystyrene with the size of 15 μm and Jurkat cells are shown in Figure 6. Average masses of a polystyrene microparticles at the size of 15 μm were measured as 8.3×10^{14} Da which are in good agreement with the calculated mass of 1.1×10^{15} Da. The full width at half-maximum of mass (Δm) for 15 μm polystyrene was measured as 5.1×10^{14} Da. Distribution of the number of charges with a peak at 40 000 is also shown in Figure 6b1.

In addition to the measurement of polystyrene microparticles, we also applied this method to measure mass distribution of Jurkat cells. The mass peak position and the charge number of Jurkat were determined as 4.6×10^{13} Da and ~17 000, respectively (Figure 6, parts a2 and b2).

As shown in Figure 6, we observed many charges (~100 000 electrons) on a cell or microparticle in an ion trap mass spectrometer. It should be interesting to explore the relationship between the number of charges a particle can carry and the mass of the particle. The relationship between the measured mass and charges of the polystyrene spheres and cells is shown in Figure 7. The number of charges on a microparticle almost has a linear relationship with the mass for the mass of particles less than 1×10^{15} Da (Figure 7). From this result, it can be estimated that the smallest particle that can be measured is about 1 μm due to the electronic background. Recently, Fuerstenau et al. reported the observation of electronic noise level equivalent to 100 electrons.[17,18] With a cooling on the detector electronics, the noise level can possibly be reduced by a factor of 5 to reach ~100 electrons for our facility. Gamero-Castano also reported a background noise of 91 electrons employing a multiple stage induction charge detector.[19] With this noise level of ~100 electrons, submicroparticle detection by CMCMS can become feasible.

It is always useful to know the mass resolution of a mass spectrometer. Whitten et al.[20] and Georlinger et al.[21] reported the

(17) Fuerstenau, S. D. *J. Mass. Spectrom. Soc. Jpn.* **2003**, *51*, 50−53.
(18) Fuerstenau, S. D.; Benner, W. H. *Rapid Commun. Mass Spectrom.* **1995**, *9*, 1528−1538.
(19) Gamero-Castano, M. M. *Rev. Sci. Instrum.* **2007**, *78*, 043301(1−6).

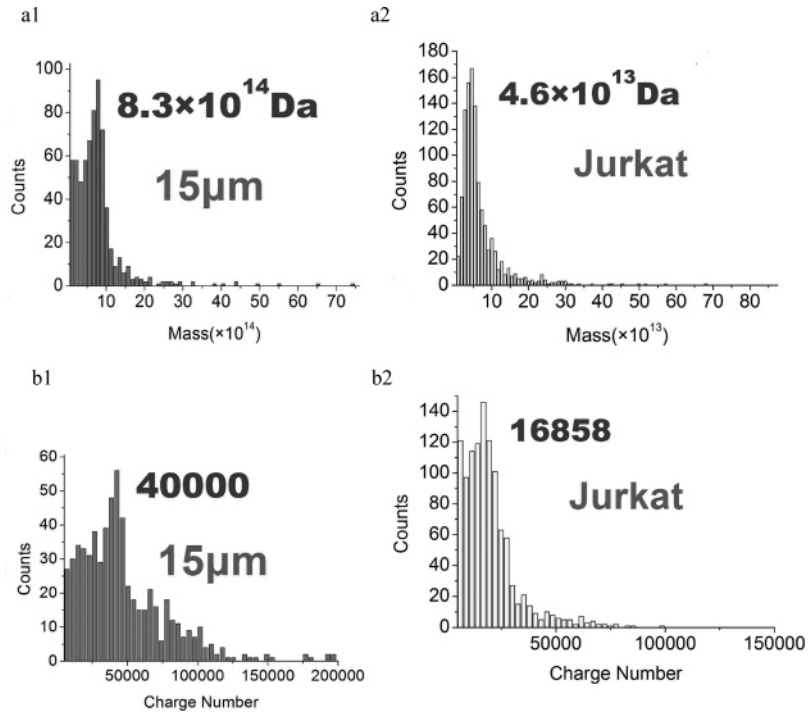

Figure 6. Histogram of mass (a1 and a2) and charge (b1 and b2) for a polystyrene sphere of 15 μm and Jurkat cancer cell.

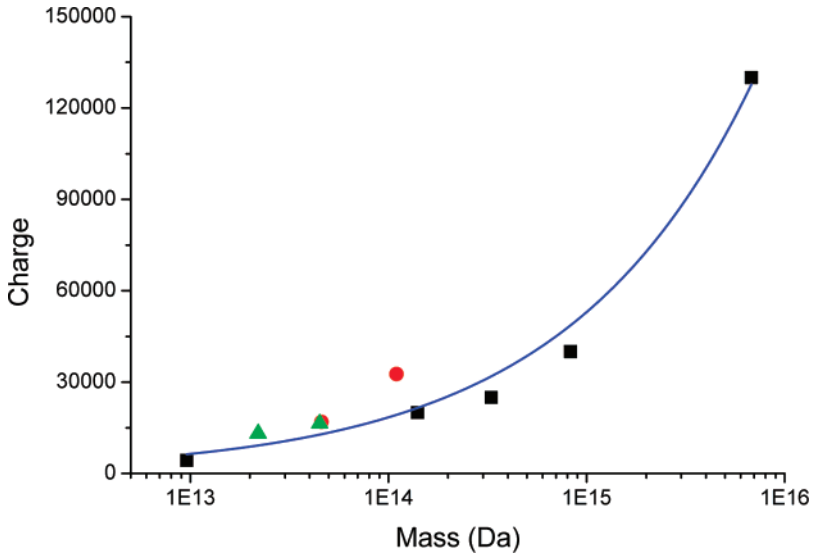

Figure 7. Averaged charge distribution vs mass of five polystyrene spheres (black squares), two normal T-cells (green triangles), and two cancer cells (red circles).

pressure effect on the mass resolution of an ion trap with resonance ejection. Up to now, few studies have been pursued on the resolution for microparticles measured under an axial mass-selective instability mode by scanning trap-driving frequency. Since it is very difficult to get a microparticle sample with small enough size distribution, a true mass resolution is difficult to obtain. Nevertheless, a sample of polystyrene microparticles with the size as 3 μm and size distribution of less than 1% was obtained from NIST (SRM 1692). The overall mass resolution is estimated as ~4. In the case with the 3 μm particles, we have recorded charge number ranging from 2000 e to slightly larger than 7000 e. This range of charge should result an uncertainty between 7% and 25% with charge detector noise of 500 e. In Figure 8, we have taken data from the 3 μm particles made two histograms using particles in different charge ranges. These plots clearly indicated the effect of charge detector noise to the mass resolution. We also did the calibration of collection time and found the mass resolution improved with the correction of the collection time (see Figure 8b).

The mass spectrometer working at high pressure is increasing its importance.[16,22] A conventional charge amplification device such

(20) Whitten, W. B.; Reilly, P. T.; Ramsey, J. M. *Rapid Commun. Mass Spectrom.* **2004**, *18*, 1749−1752.

(21) Georlinger, D. E.; Whitten, W. B.; Ramsey, J. M.; McLuckey, S. A.; Glish, G. L. *Anal. Chem.* **1992**, *64*, 1434−1439.

(22) Pau, S.; Pai, C. S.; Low, Y. L.; Moxom, J. P.; Reilly, T. A.; Whitten, W. B.; Ramsey, J. M. *Phys. Rev. Lett.* **2006**, *96*, 120801 (1−4).

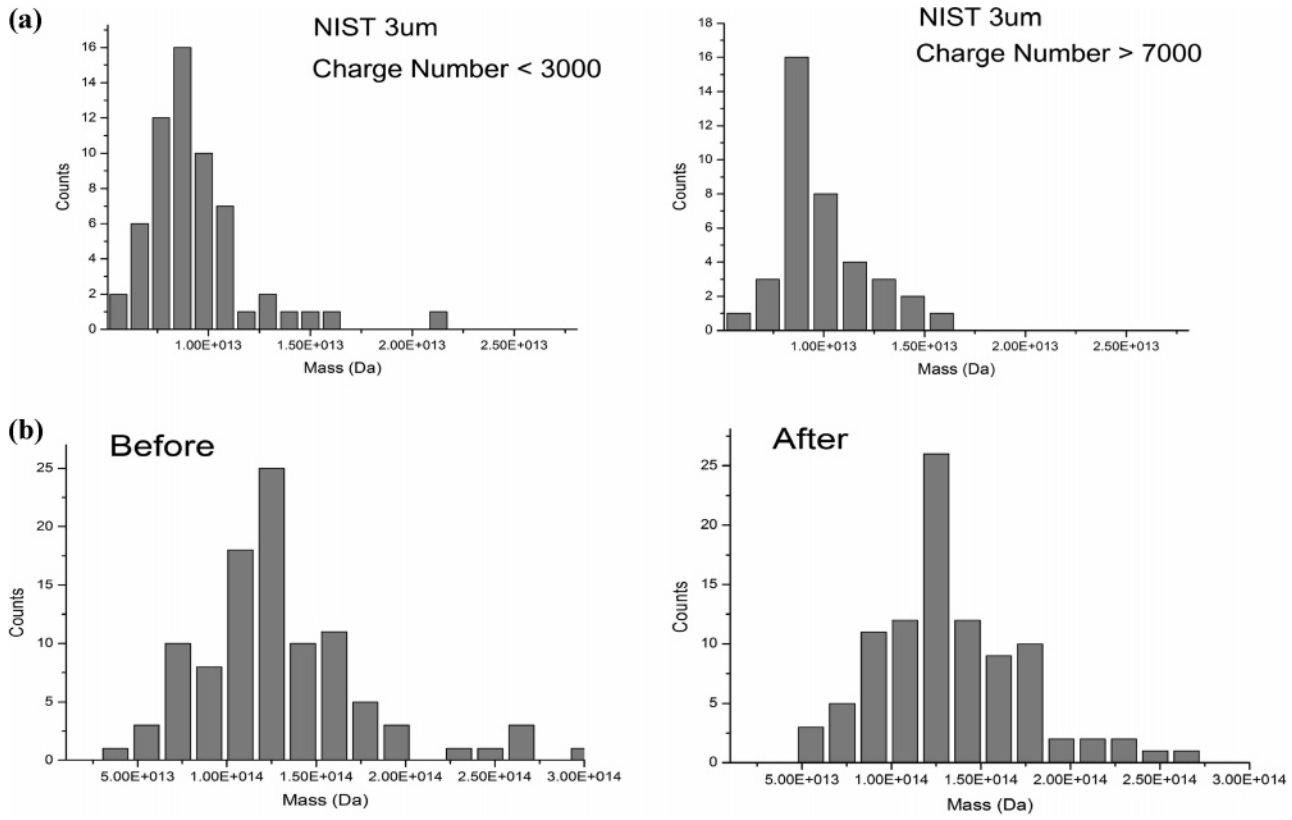

Figure 8. Mass distribution measurements (a) with different charge numbers and (b) with and without correction of charge detection efficiency due to different rise times.

as an MCP or an electron multiplier or a channeltron cannot work well at high pressure due to the discharge from the high voltage at the detector. CMCMS has demonstrated the ability of rapid mass measurement of cells, microparticles, and small molecules at relatively high buffer gas pressure of ~0.1 Torr.[15] In the future, this arrangement might have advantages to couple the charge detector for an atmosphere pressure ion source to reduce the size of a mass spectrometer for convenient transportation to the field for real-time and in situ measurements.[23,24]

CONCLUSIONS

Charge monitoring cell mass spectrometry (CMCMS) has been developed for rapid measurement of mass and mass distribution of cells and microparticles. Controlled discharge can enhance the number of charges on a microparticle to increase the accuracy of mass measurement by CMCMS. Since CMCMS can be operated at a relatively higher pressure, the lower demand on pumping can make it more feasible for field measurement in the future. This technology could be very useful in biomedical science such as mass measurement of stem cells. It can also be an interesting supplement to the aerosol mass spectrometer in conducting aerosol mass measurement.

ACKNOWLEDGMENT

This work was supported by the Genomic Research Center, Academia Sinica. Special thanks are given to Professor Y. T. Lee for valuable suggestions.

Received for review November 28, 2007. Accepted February 1, 2008.

AC7024392

(23) Patterson, G. E.; Guymon, A. J.; Riter, L. S.; Everly, M.; Griep-Raming, J.; Laughlin, B. C.; Ouyang, Z.; Cooks, R. G. *Anal. Chem.* **2002**, *74*, 6145−6153.

(24) Gao, L.; Song, Q.; Patterson, G. E.; Cooks, R. G.; Ouyang, Z. *Anal. Chem.* **2006**, *78*, 5994−6002.